Zagazig University Medical Journal
www.zumj.journals.ekb.eg
https://doi.org/10.21608/zumj.2022.173661.2684 Volume 29, Issue 4, Jully 2023

Manuscript ID ZUMJ-2211-2684 (R1)
DOI 10.21608/zumj.2022.173661.2684

ORIGINAL ARTICLE

Paeonol Preconditioning Alleviates Partial Hepatic Ischemia/Reperfusion Injury in Rats: The Role of Inhibition of Autophagy and TLR4/MyD88/NF-κB Pathway

Ahmed Ahmed Abdelsameea[1*], Amira Ebrahim Alsemeh[2], Maha K. Desouky[3], Walaa Samy[4], Amal fawzy[4], Noha A.T. Abbas[1]

[1]*Department of Pharmacology, Faculty of Medicine-Zagazig University, Zagazig, Egypt .*
[2]*Department of Human Anatomy and Embryology, Faculty of Medicine-Zagazig University, Zagazig, Egypt*
[3]*Department. of Anatomy, Faculty of Medicine, Minia University, Egypt*
[4]*Medical Biochemistry Department, Faculty of Medicine-Zagazig University, Zagazig, Egypt*

***Corresponding author:**
Ahmed A. Abdelsameea
Department of Pharmacology, Faculty of Medicine-Zagazig University, Zagazig
ahmedma_72@yahoo.com

Submit Date 2022-11-09 07:01:07
Revise Date 2022-11-12 16:02:02
Accept Date 2022-11-14

ABSTRACT

Background: Liver injury due to ischemia/reperfusion (I/R) is a major challenge during liver surgery. Effects of paeonol pretreatment on partial hepatic I/R injury were assessed in this study. **Methods:** Male Wistar rats were allocated into sham, vehicle-I/R, and paeonol-I/R groups. Paeonol, 100 mg/kg/day, was administered by gavage. After 10 days, rats of I/R groups were subjected to partial I/R of the liver. Blood samples were collected for assessment of alanine and aspartate aminotransferases as well as gamma glutamyl transferases. Liver samples were taken for detection of tumor necrosis factor-α (TNF-α) and malondialdhyde (MDA) levels as well as superoxide dismutase (SOD) activity. The mRNA expression of toll-like receptor-4 (TLR4), myeloid differentiation factor 88 (MyD88), high mobility group box 1 (HMG-1), and peroxisome proliferator-activated receptor-γ (PPAR-γ) were assessed in the liver. Hematoxylin& eosin stained liver sections were examined. Expressions of nuclear factor kappa B (NF-κB) and autophagy markers (LC3 II, P62) were assessed in immunostained sections. **Results:** Liver I/R increased serum transferases and tissue MDA, TNF-α, TLR4, HMGB-1, MyD88, NF-κB, LC3 II, P62 levels with hydropic degeneration and cellular infiltration in the liver while decreased SOD activity and PPAR-γ mRNA expression. These alterations were attenuated by paeonol pretreatment. **Conclusions:** Paeonol pretreatment alleviated liver I/R injury through inhibition of autophagy and TLR4/MyD88/NF-κB pathways.

Keywords: Reperfusion; Autophagy; Oxidative stress; Paeonol; Ischemia

INTRODUCTION

Liver injury due to ischemia/reperfusion (I/R) usually happens during liver surgery or transplantation with high morbidity and mortality sequelae [1]. Initially, hypoxia and nutrient deficiency induce hepatic injury, then reperfusion causes oxidative stress and inflammation with release of numerous mediators yielding more damage to the liver tissue [2]. Therefore, liver injury attributed to I/R requires effective preventive measures to improve liver surgery outcome.

Interplay between numerous sinusoidal, endothelial, and inflammatory cells takes place during I/R of the liver [3]. The detrimental inflammatory response to I/R injury is partially explained by activation of toll-like receptor type 4 (TLR4) signaling cascade. The high-mobility group box protein B1 (HMGB1) is a TLR4 ligand that activates TLR4 resulting in myeloid differentiation factor 88 (MyD88) activation. The latter will activate the nuclear factor kappa B (NF-κB**)** with subsequent increased expression of tumor necrosis factor-α (TNF-α) [4]. The signaling cascade involving MyD88/NF-κB activation followed by enhanced formation and release of TNF-α has an important role in the inflammatory response to I/R of the liver [5].

Autophagy is a cellular homeostatic process by which the damaged proteins and old cell organelles are processed in the autophagosome yielding substrates for resynthesis new organelles [6]. Although it is energy saving process, excessive

autophagy during stressful conditions, like I/R injury, results in a terrible degradation of essential proteins and organelles with subsequent necrosis and tissue damage [7]. Light chain 3 (LC3), a microtubule-associated protein, and P62, an autophagy receptor, are routine autophagy markers. LC3-II is a membrane-bound protein formed on the surface of autophagosome. P62 receptor is activated by LC3-II binding leading to engulfment and processing of the proteins and cell organelles [8].

Paeonol, a phenolic compound, is obtained from Paeonia lactiflora Pall roots [9]. The curative effects of paeonol in neuralgia, dermatitis, myositis, and arthritis have been reported [10]. The abovementioned clinical conditions were improved by paeonol treatment due its anti-inflammatory actions [11]. The antioxidant and anti-inflammatory effects of paeonol have been reported in many organs including the lung [12], stomach [13], brain [14], and heart [15].

This study aimed to evaluate the effect of paeonol preconditioning on the experimental partial liver I/R injury and to detect the potential mechanistics involved.

METHODS

Animals

Male Wistar rats (230–260 g) were obtained from the Faculty of Veterinary animal farm, Zagazig, Egypt. Rats were kept in animal house under standard conditions with free access to food and water. The protocols of the study were reviewed by Zagazig University-IACUC committee and attained its approval (ZU-IACUC Number: 3/F/79/2022& Date: 27 June 2022).

Drugs

Paeonol, Sigma-Aldrich (St. Louis, MO, US). Carboxy-methylcellulose: El Gomhoreya Company, Egypt. Thiopental sodium 500mg vial, EIPICO, Tenth of Ramadan City, Egypt.

Partial hepatic I/R model

About 70% of the liver mass was subjected to I/R. Under thiopental, 50mg/kg [16], anesthesia, midline abdominal incision was done followed by falciform ligament cutting to explore the portal triade of the left and median lobes (70% of the liver) which was clamped with non-traumatic clamp to induce ischemia for half an hour followed by clamp release to allow reperfusion for two hours [17]. Blood samples were withdrawn from the aorta and serum was separated for biochemical assays. The left lobe of the liver was divided into two equal sets; one was merged in liquid nitrogen then stored at −80 ˚C to be processed for biochemical studies while the other one was fixed in formalin (10%) solution for immunohistochemical and histological studies.

Experimental protocol

Three groups, six rats per each, were utilized in the study. Sham, vehicle-treated I/R (administered carboxymethylcellulose 0.5% solution 1mL/kg by gavage once daily), and paeonol-treated I/R groups. In the last group, paeonol suspended in 0.5% carboxymethylcellulose solution was administered 100mg/kg/day orally to rats [18]. In all groups, treatments were continued for 10 days. By the 10th day, rats of I/R groups underwent partial hepatic I/R, while rats of sham group were operated like I/R groups except for portal triade clamping.

Measurement of liver enzymes

Level of alanine aminotransferase (ALT), gamma glutamyl transferase (GGT) and aspartate aminotransferase (AST) in serum were determined by spectrum diagnostic kits [19& 20].

Measurement of hepatic lipid peroxidation

Malondialdhyde (MDA) level in liver homogenate was measured by thiobarbituric acid reactive substances assay kit [21].

Measurement of superoxide dismutase (SOD) activity

Inhibition of pyrogallol auto-oxidation method was utilized for assessment of SOD activity [22].

Measurement of concentration of tumor necrosis factor-alpha (TNF-α)

TNF-α level in liver homogenate was detected by rat TNF-α ELISA kit [23].

Gene expression analysis

I. **Sample preparation and cDNA synthesis**

Following instructions in the manufacturer's protocol, the total RNA was isolated from liver tissue utilizing RNA isolation kit. The RNA purity and integrity were assessed by spectrophotometer at 260/280 nm. The RNA was reverse transcribed by Reverse Transcription Kit to obtain the complementary DNA (cDNA). The latter was stored at −20°C until analysis.

II. **Measurement of mRNA expression of TLR4, HMGB1, MyD88, and PPAR-γ by RT-PCR**

StratageneMx3005P-qPCR System was used for TLR4, HMGB1, MyD88, and PPAR-γ mRNA assessment utilizing the real time polymerase chain reaction (RT-PCR). Analysis of gene expression was done by qRT-PCR. The cDNA polymerase chain reactions were performed in 20 µL of final volume (containing 50 ng cDNA); 10 pmol/uL of each primer (1 uL each), 10 uL of SYBR Green 2x Master Mix Green. The amplification was done by initial enzyme activation at 95°C for 15 min,

followed by 40 cycles of 95°C for 15 sec and then 60°C for 1 min and final extension at 72°C for 30 sec. B-actin gene was used as an internal control. The primers used for real-time PCR were reported in table (1).

Histological evaluation of the liver histoarchitecture changes by H&E stain

The formalin fixed liver tissues were dehydrated utilizing increasing alcohol grades, and then paraffin blocks were done. Slices with 5 µm thickness were stained with H&E. Scoring of hydropic degeneration were evaluated as 0 for absent, 1 for less than 25%, 2 for 25-50%, and 3 for more than 50% of degeneration. Scoring of cellular infiltration scores were calculated as 0 for absent, 1 for less than 1/3, 2 for 1/3–2/3, and 3 more than 2/3 of portal tracts infiltrated with inflammatory cells [24].

Immunohistochemical analysis for assessment of NF-κB (p65) protein and autophagy markers (LC3-II& P62)

Liver sections were deparaffinized and rehydrated in sequences of ascending concentrations of ethanol. Peroxides were deactivated by 3% H_2O_2 in PBS for 15 min and incubated at 4 ˚C with rabbit polyclonal anti-NF-κB (p65), LC3A/B or SQSTM1/ p62 Rabbit mAb overnight. The secondary antibody and avidin–biotin complex then added for 30 min. The color was generated after adding diaminobenzidine. Image J software plugin, immunohistochemistry profiler was utilized to compute positive nuclear expression (brown color).

Histopathological and immunohistochemical studies were done by two experimenters blind to the experimental groups

Statistical analysis

The obtained results were statistically analyzed by SPSS version 16 software package for Windows. One-way ANOVA followed by post hoc Tukey test was used for multiple comparisons of the parametric data, while Dunnett T3 test was utilized for multiple comparisons of non-parametric data. The statistical significance was set at $p < 0.05$.

RESULTS

ALT, AST, and GGT assessment

Liver I/R significantly ($p<0.001$) increased serum ALT, AST and GGT levels compared to sham group. Paeonol pretreatment significantly ($p<0.001$) decreased ALT, AST and GGT levels in comparison to vehicle-treated I/R group while compared to sham group ALT was significantly ($p<0.05$) increased but AST and GGT were insignificantly ($p= 0.942$ and 0.099 respectively) increased (Table 2).

SOD, MDA and TNF-α Assessment

Liver I/R significantly ($p<0.001$) decreased SOD activity compared to sham group. Paeonol pretreatment significantly ($p<0.001$) increased SOD activity compared to vehicle-treated I/R group and significantly ($p<0.05$) decreased compared to sham group.

Liver I/R significantly ($p<0.001$) increased the MDA and TNF-α concentrations compared to sham group. These levels were significantly ($p<0.001$) decreased by paeonol pretreatment compared to vehicle-treated I/R group while were insignificantly ($p=0.179$& 0.381 respectively) increased compared to sham group (Table 2).

Effect of paeonol on alterations of hepatic HMGB-1, TLR4, MyD88, and PPAR-γ mRNA expression induced by liver I/R

The hepatic mRNA expressions of TLR4, HMGB-1, and MyD88 were significantly ($P<0.001$) increased by I/R while PPAR-γ was significantly ($P<0.001$) decreased compared to sham group. Paeonol pretreatment significantly ($P<0.001$) decreased TLR4, HMGB-1, and MyD88 m RNA expressions and significantly ($P<0.05$) increased PPAR-γ compared to the vehicle-treated I/R group (Table 3).

Effect of Paeonol on liver I/R induced histopathological alterations (Table 4)

H&E-stained liver tissue from experimental groups is illustrated in Fig. 1-3. Sham group sections showed normal liver architecture without any pathological changes **(Fig. 1).** Vehicle-treated I/R group sections displayed most hepatocytes with vacuolated cytoplasm and pyknotic nuclei with hydrobic degeneration and mono cellular infiltrations scores significantly ($P<0.05$) increased in comparison to sham group, as well as dilated and congested blood sinusoids with bile duct proliferation **(Fig.2).** The paeonol-treated I/R group sections showed most hepatocytes with acidophilic cytoplasm and vesicular nuclei, but still displayed pyknotic nuclei and less vacuolated cytoplasm in some hepatocytes. The hydrobic degeneration and cellular infiltrations scores significantly ($P<0.05$) decreased in comparison to vehicle-treated I/R group **(Fig. 3).**

Effect of Paeonol-on NF-κB (p65) immunoexpression

As shown in **fig. 4**, immunohistochemical NF-κB (p65) protein staining was marked in vehicle-treated IR group while, sham group showed negative

staining. In paeonol-treated IR group, few hepatocytes' nuclei exhibited positive expression of NF-κB (p65). The number of NF-κB (p65) immune-positive nuclei is significantly (P<0.001) increased in vehicle-treated I/R group compared to sham group. However, in paeonol-treated I/R group, the number of NF-κB (p65) positive nuclei was significantly (P<0.001) decreased in comparison to vehicle-treated I/R group but still displayed a significant (P<0.05) increase as compared to sham group.

Effect of paeonol on autophagy markers immunoexpression

The immunoexpressions of autophagy related LC3-II and p62 proteins in hepatic tissue (brown staining of hepatocytes' cytoplasm) are illustrated as in **Fig. 5& 6** respectively. The percentage of LC3-II and p62 immunoexpressions are significantly (P<0.001) increased by I/R compared to sham group. LC3-II and p62 immunoexpression are significantly (P<0.001) decreased by paeonol pretreatment compared to vehicle-treated I/R group but compared sham group; LC3-II was insignificantly (p=0.066) increased while P62 displayed a significant (P<0.05) increase.

Table 1: Primer sequences of HMGB-1, TLR4, MyD88, and PPAR-γ genes

	Forward primer	Reverse primer
TLR4	GCTTTCAGCTTTGCCTTCAT	TACACCAACGGCTCTGGATA
HMGB-1	TCAGATACAAGGAAAGCGGAT	AAATTGCCAAATTGTTCCCT
MyD88	TGGTGGTTGTTTCTGACGAT	GATCAGTCGCTTCTGTTGGA
PPAR-γ	CATACATAAAGTCCTTCCCGCTG	TTGTCTGTTGTCTTTCCTGTCAAGA
β-actin	ACTGGCATTGTGATGGACTC	CAGCACTGTGTTGGCATAGA

Table 2: Effect of paeonol on alterations of ALT, AST, GGT, SOD, MDA, and TNF-α levels induced by partial liver I/R in rats

	Sham	Vehicle-treated I/R	Paeonol-treated I/R	F
ALT (U/L)	13.66±3.26	58±6.22*	21.66±2.58*#	179.014
AST (U/L)	78.66±2.20	170 ± 13.69*	80.50±8.01#	118.242
GGT (U/L)	1.54±0.52	4.25±0.73*	2.28±0.41#	43.108
SOD (U/g)	140± 12.98	53± 6.80*	114±9.30*#	118.580
MDA (μmol/g)	8.29±0.93	19.16± 1.72*	9.83± 1.47#	103.695
TNF-α (pg/g)	8.36±0.89	17.35± 2.26*	9.60±1.17#	58.183

Values represent mean ± standard deviation. *Significant from sham group. #Significant from vehicle-treated IR group. Number= 6 rats per each group. I/R: ischemia/reperfusion, ALT: alanine aminotransferase, AST: aspartate aminotransferase, GGT: γ glutamyl transferase, SOD: superoxide dismutase, MDA: malondialdhyde. TNF-α: tumor necrosis factor-alpha. F=variation between sample means / variation within the samples.

Table 3: Effect of paeonol on alterations of hepatic HMGB1, TLR4, myD88, and PPAR-γ mRNA expression levels induced by liver I/R in rats

	Sham	Vehicle-treated I/R	Paeonol-treated I/R	F
TLR4	1.09±0.11	2.31±0.23*	1.35±0.15*#	81.84
HMGB1	1.12±0.07	2.73±0.19*	1.44±0.12*#	230.66
MyD88	1.11±0.14	3.14±0.27*	1.87±0.18*#	141.56
PPAR-γ	1.08±0.13	0.56±011*	0.87±0.14*#	23.74

Values represent mean ± standard deviation. *Significant from sham group, # significant from vehicle-treated I/R group. Number= 6 rats per each group. I/R: ischemia/reperfusion, HMGB1: High mobility group box 1, TLR-4: Toll-like receptor, MyD88: Myeloid differentiation factor88, PPAR-γ: Peroxisome proliferator-activated receptor-gamma. F=variation between sample means / variation within the samples

Table 4: Hydropic degeneration and cellular infiltration scores in hepatic tissues of sham, vehicle-treated IR, and paeonol-treated I/R groups

Groups	Sham	Vehicle-treated IR	Paeonol-treated I/R	F
Hydropic degeneration score	0.0±0.0	2.33±0.81*	0.50±0.54*#	28.10
Cellular infiltrations score	0.0±0.0	1.66±0.51*	0.33±0.51*#	26.25

Values represent mean score± standard deviation. * Significant from sham group, # Significant from vehicle-treated IR group. Number = 6 rats per each group. I/R: ischemia/reperfusion. F=variation between sample means / variation within the samples

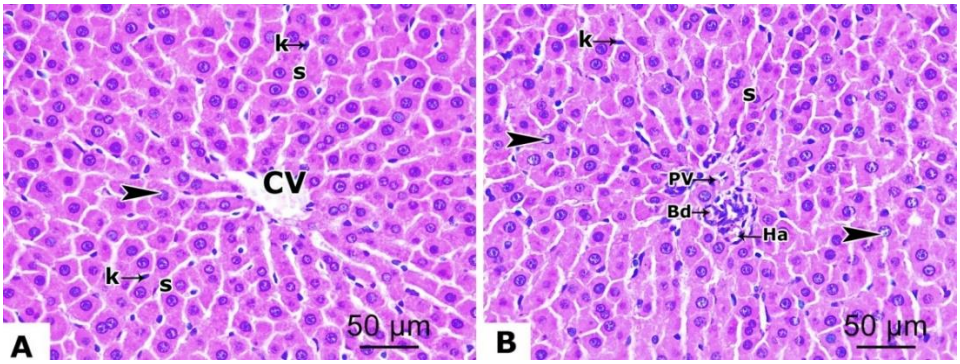

Figure 1: (A, B) Photomicrographs of liver tissues stained with H&E from sham group. These sections show hepatocytes with acidophilic cytoplasm (arrow heads), central vein (CV), the portal vein (PV), hepatic artery (Ha), bile duct (Bd) and separated by blood sinusoids (s) with Kupffer cells. Scale bar= 50 µm, x400

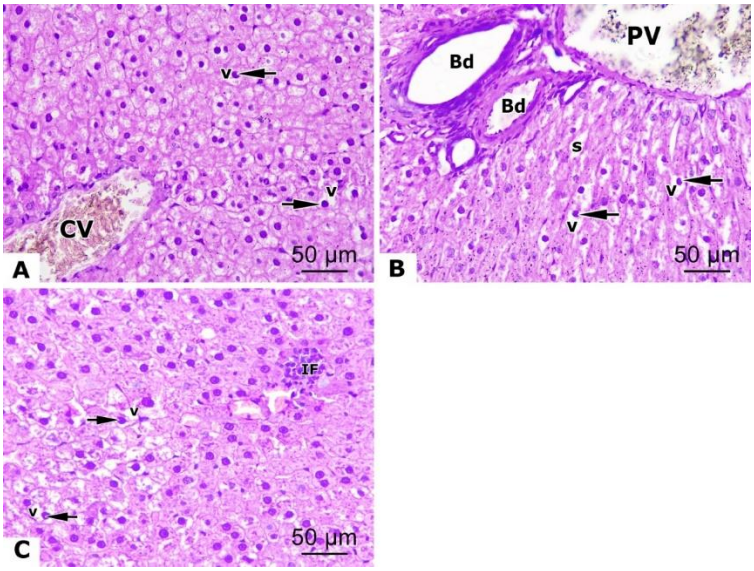

Figure 2: (A,B&C) Representative photomicrographs of liver tissues sections stained with H&E from vehicle-treated I/R group. These sections show disrupted architecture with dilated and congested central (CV) and portal (PV) veins. Most hepatocytes have pyknotic nuclei (short arrow) and vacuolated cytoplasm (v) and separated by dilated blood sinusoids (S*). Bile duct proliferation (Bd) and mono cellular infiltrations (IF) can be observed. Scale bar= 50 µm, x400

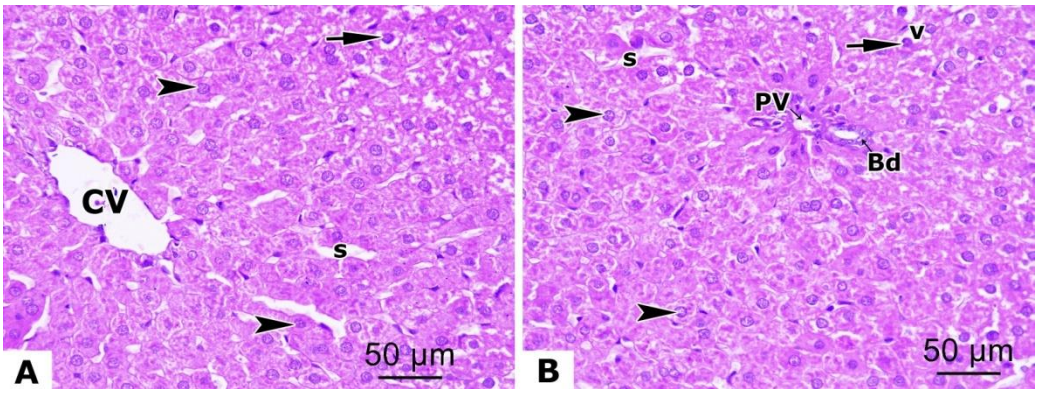

Figure 3: (A, B) Photomicrographs of H&E-stained liver tissue sections of paeonol-treated I/R group revealed restoration of the most of normal appearance of hepatocytes with slightly dilated central vein (CV). Most hepatocytes with acidophilic cytoplasm and rounded vesicular nuclei (arrowhead) and separated by slightly dilated blood sinusoids (S*), few scattered hepatic cells with pyknotic nuclei (short arrow) and vacuolated cytoplasm (v) can be noticed around the central vein (CV) and the portal vein (PV). Bile duct (Bd) can be seen.

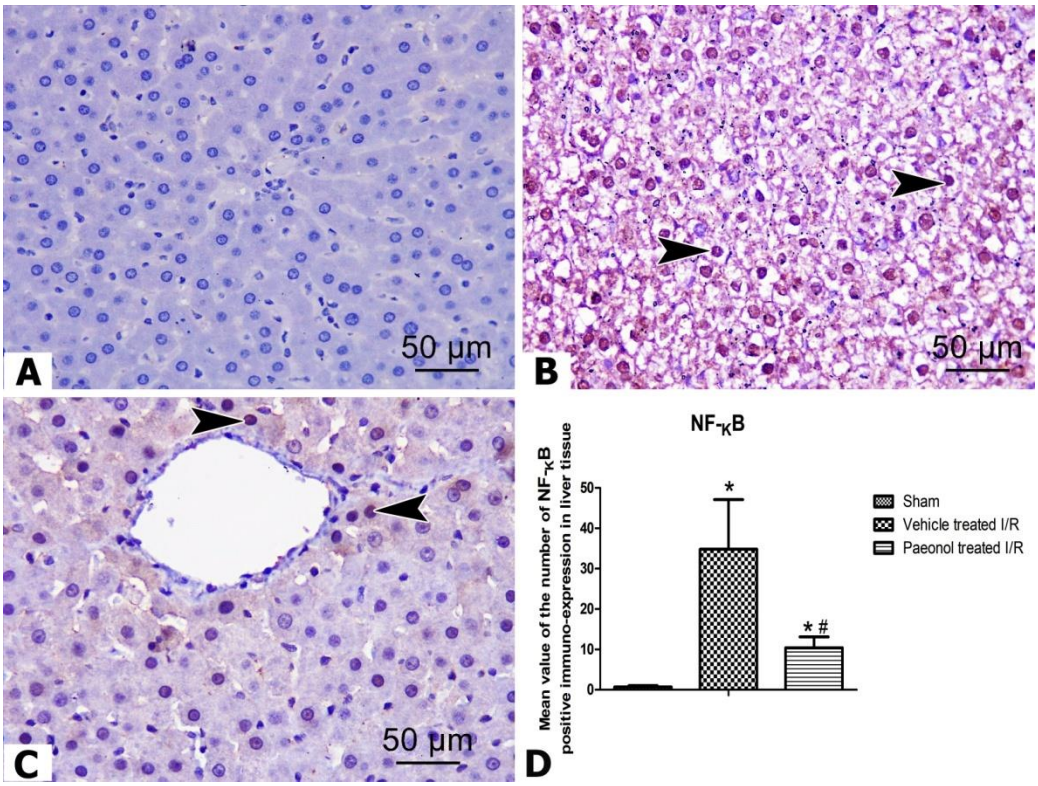

Figure 4: Microscope images represent NF-κB (p65) immunostained sections in the studied group. Sham group (A) shows no positive immunostained cells while vehicle-treated I/R group (B) shows strong positive brown staining (nuclear reaction). Paeonol-treated IR group (C) shows marked decrease in positive brown reaction. The arrowhead points to positive immunostained cells. (D) A bar chart displays the mean and standard deviation of number of NF-κB (p65) positive cells in the studied groups. *Significant from sham group, #Significant from vehicle-treated IR group, F= 137.842. I/R: ischemia/reperfusion

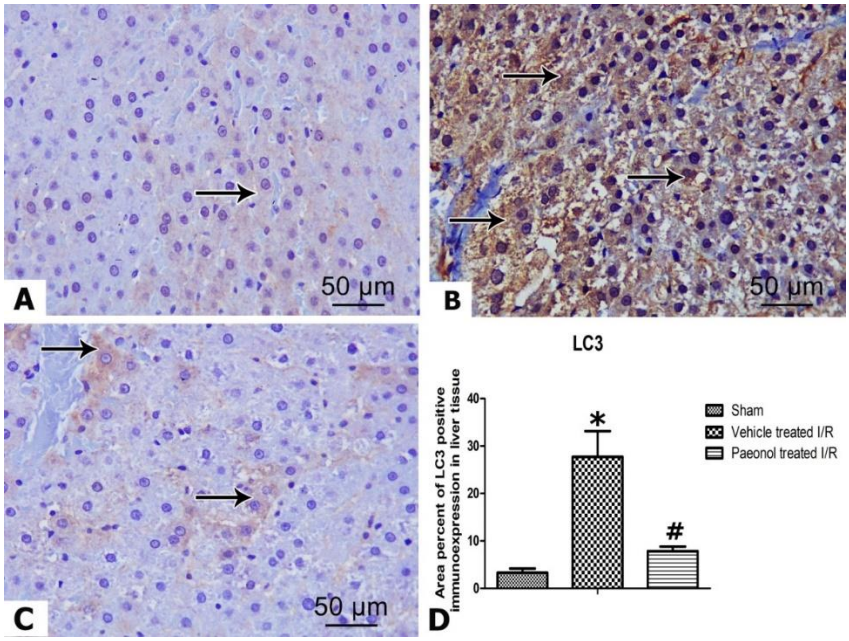

Figure 5: Representative microscopic images show immunohistochemical staining of autophagy associated protein LC3-II among (A) sham, (B) vehicle-treated I/R and (C) paeonol-treated I/R groups. Arrow refers to the brown staining of the cytoplasm of the hepatocytes that indicates the positive immunoexpression of LC3. (D) A bar chart represents the mean and standard deviation of the area % of LC3 immunoexpression among the studied groups. *Significant from sham group, #Significant from vehicle-treated I/R group, F= 96.707. I/R: ischemia/reperfusion

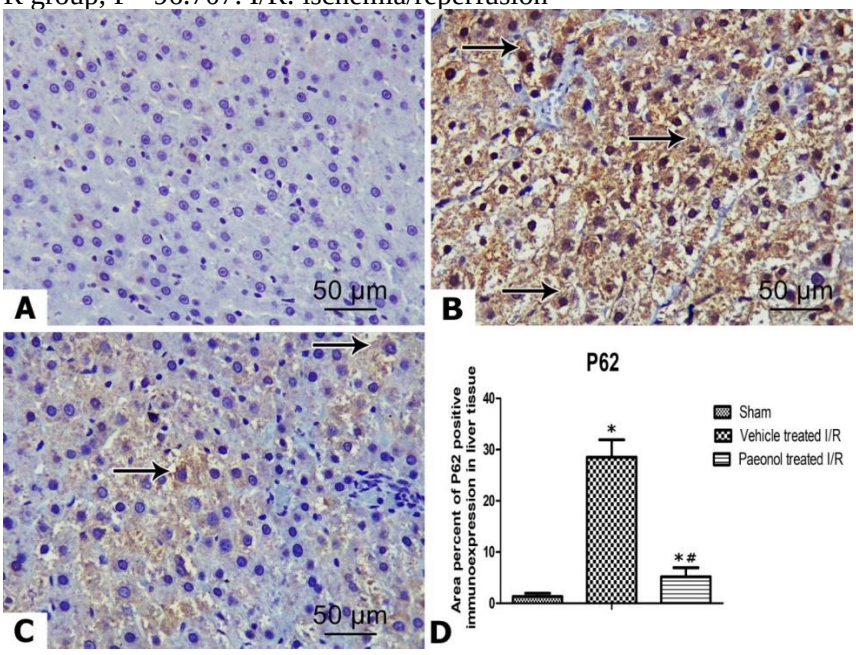

Figure 6: Representative microscopic images show immunohistochemical staining of autophagy associated protein P62 among (A) sham, (B) vehicle-treated I/R, and (C) paeonol-treated I/R groups. Arrowhead refers to the brown staining of the cytoplasm of the hepatocytes that indicates the positive immunoexpression of P62. (D) A bar chart represents the mean and standard deviation of the area % of P62 immunoexpression among the studied groups. * Significant from sham group, # Significant from vehicle-treated IR group, F= 254.297. I/R: ischemia/reperfusion.

DISCUSSION

The liver tissue damage following I/R yields a marked disturbance in the liver functions [25]. The extent of hepatic damage is usually correlated with increases in serum aminotransferases concentrations [26]. In this study, serum levels of aminotransferases were elevated by I/R of the liver**,** while paeonol preconditioning attenuated these elevations. As ALT, AST and GGT are intracellular enzymes; increments in their serum levels after reperfusion indicate necrosis of liver tissue [27]. The biochemical findings in the current study were confirmed by the histopathological findings which showed hepatocyte hydropic degeneration after I/R.

In this work, the biochemical and histopathological alterations resulted from I/R injury were attenuated by paeonol preconditioning. Indeed, the protective effects of paeonol were documented in experimental I/R injury in other organs. In this context, paeonol decreased size of infarction in rat model of cerebral I/R injury [28]. In addition, paeonol was reported to alleviate the myocardial I/R injury in rats [29].

The reperfusion injury generates reactive oxygen species (ROS) which interact with the hepatocyte membrane lipids leading to lipid peroxidation with subsequent necrosis [30]. While, MDA is a marker of lipid peroxidation, SOD has a protective effect against ROS-induced damage [31]. In these results, MDA level was increased with exhausted SOD activity following I/R of the liver. Interestingly, paeonol protected hepatocyte membrane from lipid peroxidation; these effects were documented by MDA decrement and SOD enhancement. The antioxidant effects of paeonol were previously documented by increasing SOD activity and decreasing MDA level in rats with hepatic carcinoma [32].

In the present findings, I/R injury of liver induced detrimental inflammatory response. The latter was attenuated by paeonol pretreatment. In this context, the level of TNF-α was increased by I/R injury, while paeonol pretreatment attenuated this increase. An interplay exists between ROS, TNF-α and NF-κB pathway during I/R injury of the liver. This was documented by increased leukocyte chemotaxis and ROS generation by TNF-α [33], while NF-κB enhanced gene expression of TNF-α and IL-1 during I/R of the liver [34]. In addition, neutralization of TNF-α was reported to decrease I/R injury of the liver [35]. In parallel with the present findings, paeonol treatment was found to reduce TNF-α in hepatocellular carcinoma rats [32]**.** Moreover, it ameliorated vascular inflammation via suppression of NF-κB pathway [36].

As TLR4 activation enhances inflammatory cytokines production, suppression of TLR4 signaling pathway might be a target in mitigation of I/R injury [37]. The pathogenesis of I/R injury resides partially in HMGB-1/TLR4 axis activation [38]. In this work, TLR4 and HMGB-1 expressions were increased by liver I/R while, paeonol pretreatment prevented these increments. Indeed, Andrassy [39] found that, HMGB-1 neutralization with or without TLR4 blockade exerted anti-inflammatory effects with subsequent myocardial I/R injury attenuation. In addition, it was reported that, inhibition of TLR4 signaling and the use of neutralizing antibodies to HMGB-1 protected against inflammatory injury in the hepatic I/R [40].

As regarding the intracellular adaptor molecule, MyD88, the present results showed that hepatic I/R injury increased its expression and decreased by paeonol pretreatment. MyD88 overexpression was reported to increase the inflammatory cytokines such TNF-α and IL-1 following experimental intestinal I/R injury [41]. In addition, TLR4/MyD88/NF-κB pathway inhibition had hepatoprotective effect against liver I/R injury in mice [42]. In this work, liver I/R decreased the hepatic PPAR-γ mRNA expression. Interestingly, paeonol pretreatment counteracted this effect. The anti-inflammatory effects of PPAR-γ activation are explained by nitric oxide synthase and NF-κB inhibition as well as controlling phagocyte activity [43].

The nutritional deficiency during ischemia and oxidative stress resulted from tissue reperfusion are considered inducers of autophagy [44]. Although autophagy is a beneficial homeostatic process, over-activated autophagy is detrimental. In this study, we found that hepatic I/R injury increased LC3-II and P62 proteins expression denoting over-activation of autophagy. Meanwhile, paeonol pretreatment decreased their levels reflecting autophagy suppression. These findings coped with Tsai et al. [29] who reported that paeonol attenuated myocardial I/R injury though inhibition of autophagy.

In this study, the autophagy markers, LC 3-II and P62, were minimally expressed in sham group but overexpressed by I/R while paeonol pretreatment prevented its overexpression. Excessive autophagy was reported to worsen lung I/R injury in rats and 3-MA, a standard autophagy

inhibitor, improved lung function in this preclinical paradigm [45]. In addition, inhibition of autophagy had a good impact on renal function after kidney transplantation [46]. Moreover, experimental studies have reported that I/R injury of kidney and liver enhanced autophagy. In these organs, inhibition of autophagy successfully reduced I/R injury [47, 48].

CONCLUSIONS

Liver I/R induced detrimental oxidative, inflammatory and autophagic injuries of the hepatic tissue. Paeonol prevented I/R-induced oxidative injury via SOD enhancement and exerted anti-inflammatory effects by decreasing TNF-α through inhibition of TLR4/MyD88/NF-kB pathway with PPAR-γ enhancement. It inhibited excessive autophagy by decreasing LC3-II and P62.

Therefore, paeonol pretreatment shows potential as a preventive measure in liver surgery.

Conflicts of interest: None

Financial disclosure: None

REFERENCES

1. Costa CCC, Pereira NG, Machado ALM, Dórea MA, Cruz RMMD, Silva RC et al. Splenic ischemic preconditioning attenuates oxidative stress induced by hepatic ischemia-reperfusion in rats. *Acta Cir Bras* 2019; 34(7):e201900707. https://doi.org/10.1590/s0102-8650201 90070000007
2. Guan LY, Fu PY, Li PD, Li ZN, Liu HY, Xin MG et al. Mechanisms of hepatic ischemia-reperfusion injury and protective effects of nitric oxide. *World J Gastrointest Surg* 2014; 6(7):122–128. https://doi.org/10.4240/wjgs.v6. i7.122
3. Montalvo-Jave EE, Escalante-Tattersfield T, Ortega-Salgado JA, Piña E, Geller DA Factors in the pathophysiology of the liver ischemia-reperfusion injury. *J Surg Res* 2008; 147(1):153–159. https://doi.org/10.1016/j.jss.2007.06.015
4. Tu XK, Yang WZ, Shi SS, Wang CH, Zhang GL, Ni TR et al. Spatio-temporal distribution of inflammatory reaction and expression of TLR2/4 signaling pathway in rat brain following permanent focal cerebral ischemia, *Neurochem Res* 2010; 35:1147–1155.
5. Bauernfeind F, Horvath G, Stutz A, Alnemri ES, Speert D, Fernandes-alnemri T et al. Cutting Edge: NF kappa B Activating Pattern Recognition and Cytokine Receptors License NLRP3 Inflammasome Activation by Regulating NLRP3 Expression. *Immunol* 2009; 183:787–791. https://doi.org/10.4049/jimmunol.0901363.NF-Kb.
6. Baehrecke EH. Autophagy: dual roles in life and death? *Nat Rev Mol Cell Biol.* 2005; 6:505–510.
7. Zeng M, Wei X, Wu Z, Li W, Zheng Y, Li B. Simulated ischemia/reperfusion-induced p65-Beclin1-dependent autophagic cell death in human umbilical vein endothelial cells. *Sci Rep* 2016; 6:37448. doi:10.1038/ srep37448
8. Bento CF. Mammalian Autophagy: How Does It Work? *Annual Rev of Biochem* 2016; 85:685–713.
9. Koo YK, Kim JM, Koo JY, Kang SS, Bae K, Kim YS. Platelet anti-aggregatory and blood anti-coagulant effects of compounds isolated from Paeonia lactiflora and Paeonia suffruticosa. *Pharmazie* 2010; 65:624–628. doi:10. 1691/ph.2010.9870
10. Chen N, Liu D, Soromou LW, Sun J, Zhong W, Guo W. Paeonol suppresses lipopolysaccharide-induced inflammatory cytokines in macrophage cells and protects mice from lethal endotoxin shock, *Fundam Clin Pharmacol* 2014; 28:268–276, https://doi.org/10.1111/fcp.12019.
11. Hsieh CL, Cheng CY, Tsai TH. Paeonol reduced cerebral infarction involving the superoxide anion and microglia activation in ischemia-reperfusion injured rats. *Journal of Ethnopharmacol* 2006; 106 (2):208–215.
12. Wang F, Zhu M, Jiang N, Zhang M, Feng L, Jia X. Paeonol ameliorates lipopolysaccharides-induced acute lung injury by regulating TLR4/MyD88/NF-κB signaling pathway. *Die Pharmazie* 2019; 74(2):101–106. https://doi.org/10.1691/ph.2019.8860
13. Hafez HM, Morsy MA, Mohamed MZ, Zenhom N M. Mechanisms underlying gastroprotective effect of paeonol against indomethacin-induced ulcer in rats. *Human and Experimental Toxicology* 2019; 38(5):510–518. https://doi.org/10.1177/0960327118 818254
14. Jin H, Wang M, Wang J, Cao H, Niu W, Du L. Paeonol attenuates isoflurane anesthesia-induced hippocampal neurotoxicity via modulation of JNK/ERK/P38MAPK pathway and regulates histone acetylation in neonatal rat. *The Journal of Maternal-Fetal & Neonatal Medicine.* 2020; 33(1):81–91. https://doi.org/10.1080/14767 058.2018.1487396
15. Li H, Song F, Duan LR, Sheng JJ, Xie YH, Yang Q et al. Paeonol and danshensu combination attenuates apoptosis in myocardial infarcted rats by inhibiting oxidative stress: Roles of Nrf2/HO-1 and PI3K/Akt pathway. *Scientific Reports* 2016; 6: 23693. https://doi.org/10.1038/srep23693
16. Zorniak M, Mitrega K, Bialka S, Proc M and Krezm TS. Comparison of thiopental, urethane, and pentobarbital in the study of experimental cardiology in rats. *J Cardiovas Pharmacol.* 2010; 56(1):38-44
17. Shibamoto T, Kuda Y, Tanida M, Wang M, Kurata Y. Exercise attenuates ischemia-reperfusion injury of nonalcoholic fatty liver in OLETF rat. *Gastroenterol Pancreatol Liver Disord* 2015; 2(2):1–6.
18. Morsy MA, El-Sheikh AAK, Abdel-Hafez SMN, Kandeel M, Abdel-Gaber SA. Paeonol Protects Against Methotrexate-Induced Nephrotoxicity via Upregulation of P-gp Expression and Inhibition of TLR4/NF-κB Pathway. Front. *Pharmacol* 2022; 13:774387. doi: 10.3389/fphar.2022.774387
19. Reitman S, Frankel S. A colorimetric method for the determination of serum glutamic oxalacetic and glutamic pyruvic transaminases. *Am J Clin Pathol* 1957; 28(1):56-63.

20. Szasz B. A kinetic photometric method for serum gamma-glutamyl transferase. *Clin chem* 1969; 15(2):124-136.
21. Yagi, K. Free Radicals and Antioxidant Protocols. 1998; 108: 101-106.
22. Marklund S, Marklund G. Involvement of the suerperoxide anion radical in the autooxidation of pyrogallol and a convenient assay for superoxide dismutase. *Eur J Biochem* 1974; 47:469-474.
23. Bonavida B. Immunomodulatory effect of tumor necrosis factor. *Biotherapy* 1991; 3: 127-33.
24. Kleiner DE. Design and validation of a histological scoring system for nonalcoholic fatty liver disease. *Hepatol*. 2005; 41: 1313-1321.
25. Pérez JC, Ramírez AC, González LT, Espinosa LE, Quintana MM, Galván GA et al. Spironolactone effect in hepatic ischemia/reperfusion injury in Wistar rats. *Oxidative Med Cell Longev* 2016; 9. doi:10.1155/2016/31964313196431
26. Mard SA, Akbari G, Dianat M, Mansouri E. Protective effects of crocin and zinc sulfate on hepatic ischemia-reperfusion injury in rats: a comparative experimental model study. *Biomed Pharmacother* 2017; 96:48–55.
27. Xia H, Liu Z, Liang W, Zeng X, Yang Y, Chen P et al. Vagus nerve stimulation alleviates hepatic ischemia and reperfusion injury by regulating glutathione production and transformation. *Oxid Med Cell Longev* 2020:1079129–1079115. https://doi.org/10.1155/2020/1079129
28. Liao WY, Tsai TH, Ho TY, Lin YW, Cheng CY, Hsieh CL. Neuroprotective effect of paeonol mediates anti-inflammation via suppressing toll-like receptor 2 and toll-like receptor 4 signaling pathways in cerebral ischemia-reperfusion injured rats. *Evid Based Complement Alternat Med* 2016; 3704647: 1-12. doi:10.1155/2016/3704647
29. Tsai CF, Su HH, Chen KM, Liao JM, Yao YT, Chen YH et al. Paeonol Protects Against Myocardial Ischemia/Reperfusion-Induced Injury by Mediating Apoptosis and Autophagy Crosstalk. *Front Pharmacol* 2021; 11:586498. doi: 10.3389/fphar.2020.586498
30. Abu-Amara M, Yang SY, Tapuria N, Fuller B, Davidson B, Seifalian A. Liver ischemia/reperfusion injury: processes in inflammatory networks--a review. *Liver Transp.* 2010; 16(9):1016–1032. https://doi.org/10.1002/lt.22117
31. Freudenthaler SM, Schreeb KH, Wiese A, Pilz J, Gleiter CH. Influence of controlled hypoxia and radical scavenging agents on erythropoietin and malondialdehyde concentrations in humans. *Acta Physiol Scand* 2002; 174: 231-235
32. Chen B, Ning M, Yang G. Effect of Paeonol on Antioxidant and Immune Regulatory Activity in Hepatocellular Carcinoma Rats. *Molecules* 2012;17:4672-4683; doi:10.3390/molecules17044672.
33. Shibuya H, Ohkohchi N, Tsukamoto S. Tumor necrosis factor-induced, superoxide-mediated neutrophil accumulation in cold ischemic/reperfused rat liver. *Hepatol* 1997; 26:113.
34. Ali S, Mann DA. Signal transduction via the NF-kappaB pathway: a targeted treatment modality for infection, inflammation and repair. *Cell Biochem Funct* 2004; 22: 67-79
35. Kiuchi T, Oldhafer KJ, Schlitt HJ. Background and prognostic implications of perireperfusion tissue injuries in human liver transplants: A panel histochemical study. *Transplantation* 1998; 66:p737.
36. Yuan XJ, Chen J and Dai M. Paeonol promotes microRNA126 expression to inhibit monocyte adhesion to ox-LDL-injured vascular endothelial cells and block the activation of the PI3K/Akt/NF-κB pathway. *Internat J of Mol Med* 2016; (6): p38.
37. Zheng Y, Bua J, Yua L, Chena J, Liua H. Nobiletin improves propofol-induced neuroprotection via regulating Akt/mTOR and TLR 4/NF-kB signaling in ischemic brain injury in rats. *Biomed & Pharmacoth* 2017; 91:494–503
38. Ding HS, Yang J, Chen P, Yang J, Bo SQ, Ding JW et al. The HMGB1-TLR4 axis contributes to myocardial ischemia/reperfusion injury via regulation of cardiomyocyte apoptosis, *Gene* 2013; 527 (1):389-393
39. Andrassy M. High-mobility group box-1 in ischemia–reperfusion injury of the heart. *Circulation* 2008; 117:3216–3226.
40. Tsung A, Hoffman RA, Izuishi K. Hepatic ischemia/ reperfusion injury involves functional TLR4 signaling in nonparenchymal cells. *J Immunol* 2005; 175(11):7661–7668
41. Sukhotnik I, Ben Shahar Y, Halabi S et al. Effect of N-Acetylserotonin on TLR-4 and MyD88 Expression during Intestinal Ischemia-Reperfusion in a Rat Model. European *J of Pediat Surg* 2018; doi:10.1055/s-0037-1618593
42. Du Y, Qian B, Gao L et al. Aloin Preconditioning Attenuates Hepatic Ischemia/Reperfusion Injury via Inhibiting TLR4/MyD88/NF-κB Signal Pathway In Vivo and In Vitro. Oxidative *Med and Cellul Longev* 2019; 1–14. doi:10.1155/2019/3765898
43. Matsuyama M, Yoshimura R, Hase T, Uchida J, Tsuchida K, Takemoto Y et al. Expression of peroxisome proliferator-activated receptor-gamma in renal ischemia-reperfusion injury. *Transplant Proc* 2005; 37: 1684–1685. PMID: 15919430
44. Kassan A, Pham U, Nguyen Q, Reichelt ME, Cho E, Patel PM et al. Caveolin-3 plays a critical role in autophagy after ischemia-reperfusion. *Am J Physiol Cell Physiol* 2016; 311: C854-C865
45. Zhang J, Wang JS, Zheng ZK, Tang J, Fan K, Guo H et al. Participation of autophagy in lung ischemia-reperfusion injury in vivo. *J Surg Res* 2013; 182: e79-87.
46. Turkmen K, Martin J, Akcay A, Nguyen Q, Ravichandran K, Faubel S et al. Apoptosis and autophagy in cold preservation ischemia. *Transplant* 2011; 91: 1192-1197

47. Suzuki C, Isaka Y, Takabatake Y, Tanaka H, Koike M, Shibata M et al. Participation of autophagy in renal ischemia/reperfusion injury. *Biochem Biophys Res Commun* 2008; 368: 100-106

48. Gotoh K, Lu Z, Morita M, Shibata M, Koike M, Waguri S et al. Participation of autophagy in the initiation of graft dysfunction after rat liver transplantation. *Autophagy* 2009; 5: 351-360

To Cite:

Abdelsameea, A., Alsemeh, A., Desouky, M., Samy, W., Fawzy, A., Abbas, N. Paeonol Preconditioning Alleviates Partial Hepatic Ischemia/Reperfusion Injury in Rats: The Role of Inhibition of Autophagy and TLR4/MyD88/NF-κB Pathway. *Zagazig University Medical Journal*, 2023; (983-993): -. doi: 10.21608/zumj.2022.173661.2684